

Spontaneous Symmetry Breaking in Two-dimensional Long-range Heisenberg Model

Dingyun Yao,^{1,*} Tianning Xiao,^{1,*} Zhijie Fan,^{1,2,3,†} and Youjin Deng^{1,2,3,‡}

¹*Hefei National Research Center for Physical Sciences at the Microscale and School of Physical Sciences, University of Science and Technology of China, Hefei 230026, China*

²*Hefei National Laboratory, University of Science and Technology of China, Hefei 230088, China*

³*Shanghai Research Center for Quantum Science and CAS Center for Excellence in Quantum Information and Quantum Physics, University of Science and Technology of China, Shanghai 201315, China*

The introduction of decaying long-range (LR) interactions $1/r^{d+\sigma}$ has drawn persistent interest in understanding how system properties evolve with σ . The Sak's criterion and the extended Mermin-Wagner theorem have gained broad acceptance in predicting the critical and low-temperature (low-T) behaviors of such systems. We perform large-scale Monte Carlo simulations for the LR-Heisenberg model in two dimensions (2D) up to linear size $L = 8192$, and show that, as long as for $\sigma \leq 2$, the system exhibits spontaneous symmetry breaking, via a single continuous phase transition, and develops a generic long-range order. We then introduce an LR simple random walk (LR-SRW) with the total walk length fixed at $O(L^d)$, satisfying the extensivity of statistical systems, and observe that the LR-SRW can faithfully characterize the low-T scaling behaviors of the LR-Heisenberg model in both 2D and 3D, as induced by Goldstone-mode fluctuations. Finally, based on insights from LR-SRW, we propose a general criterion for the phase transition and the low-T properties of LR statistical systems with continuous symmetry in any spatial dimension.

Low-dimensional (low-d) physics has fundamentally advanced condensed matter research through seminal discoveries, such as the quantum Hall effect [1–3] and topological insulators [4–6]. Continuous symmetry breaking and phase transition behavior in low-d also represent a core research focus. The Mermin–Wagner (M-W) theorem establishes a criterion for the existence of long-range order (LRO) in low-d systems with continuous symmetry [7]. In dimensions $d \leq 2$, LRO cannot emerge at finite temperature (finite-T) in classical systems, and such systems exhibit no finite-T phase transition, with the exception of the Berezinskii–Kosterlitz–Thouless (BKT) transition in the two-dimensional (2D) XY model [8]. However, when long-range (LR) interactions are introduced, both the phase transition properties and low-T behaviors are significantly altered. For algebraically decaying interactions $\sim 1/r^{d+\sigma}$, the universality class of the phase transition can vary with σ . Moreover, low-d systems can indeed support LRO depending on the value of σ [9–12].

As early as 1972, Fisher employed a renormalization group (RG) approach [13] and established a threshold $\sigma_* = 2$ for LR- $O(n)$ models: when $d/2 < \sigma < \sigma_*$ (nonclassical regime), the critical exponents vary with σ ; when $\sigma \geq \sigma_*$ (short-range regime), the system reverts to its short-range (SR) universality class. Later, Sak proposed an alternative threshold, shifting the boundary to $\sigma_* = 2 - \eta_{\text{SR}}$ [14], where η_{SR} denotes the anomalous dimension for SR universality. While this threshold has gained considerable acceptance and is commonly referred to as the Sak's criterion [15–21], it has also been challenged by some numerical and theoretical results [22–24]. Thus far, no rigorous mathematical proof has been achieved.

The introduction of LR interactions can also stabilize LRO in low-d systems, which is explicitly forbidden by

the M-W theorem under SR interactions. In 2001, Bruno extended the M-W theorem [25], stating that for 1D and 2D LR-XY and LR-Heisenberg models, LRO cannot exist at finite-T when $\sigma \geq d$. This has motivated extensive theoretical, experimental, and numerical studies on systems including 1D LR ferromagnetic and antiferromagnetic Heisenberg chains [26–31], 2D LR diluted XY model [32], 2D LR quantum XY [33, 34], and Heisenberg models [31, 35, 36]. All these studies report results consistent with the extended M-W theorem.

The Sak's criterion and the extended M-W theorem describe critical and low-T properties of LR systems, respectively. However, a paradox seems to exist in the 2D LR-XY model for $7/4 \leq \sigma < 2$: the system is expected to undergo a BKT transition according to Sak's criterion, yet it exhibits LRO at low temperatures, as predicted by the extended M-W theorem. A scenario was recently proposed [37, 38]: the system first undergoes a BKT transition into a quasi-long-range order (QLRO) phase, and then enters the LRO phase via another phase transition. Nevertheless, recent studies [39, 40] provide strong numerical evidence for the absence of two distinct transitions within $7/4 \leq \sigma < 2$.

In this work, we perform large-scale Monte Carlo (MC) simulations of the 2D LR-Heisenberg model and obtain the phase diagram as shown in Fig. 1. As long as $\sigma \leq 2$, the LR-Heisenberg model exhibits spontaneous symmetry breaking and develops the generic LRO at low-T, via a single second-order phase transition. In the ordered phase, the spin-spin correlation $g(r)$ saturates to a constant $g_0 > 0$ as distance $r \rightarrow \infty$. Goldstone-mode (transverse) fluctuations induce a power-law decay as $g(r) \simeq g_0 + ar^{\sigma-d}$, well described by a Gaussian free field (GFF) in the continuum limit. For $\sigma > 2$, the SR behavior is recovered: no finite-T transition exists, and,

at low- T , the correlation length ξ diverges exponentially as the inverse temperature $\beta = 1/T$ increases – the signature of asymptotic freedom in the field-theoretical description [39]. This establishes $\sigma_* = 2$ as the threshold separating the nonclassical and SR regimes, consistent with the result for the 2D LR-XY model [39, 40]. In particular, at the marginal case $\sigma = 2$, the system does not revert to the SR universality class. Instead, it exhibits a continuous transition into an LRO phase where the correlation function displays a characteristic logarithmic saturation to a constant, as $g(r) \simeq g_0 + a/\ln(r)$ – contrary to the predictions of the extended M-W theorem.

For $O(n)$ spin models with SR interactions in high dimensions $d \geq 4$, simple random walks (SRW) are frequently employed to characterize or even prove the critical behaviors, since these systems are governed by the Gaussian fixed point in the RG framework. Specifically, SRW with an appropriately predetermined length was introduced to describe the subtle finite-size scaling (FSS) behaviors of high- d $O(n)$ systems [41–43]. To investigate the Goldstone-mode physics in low- T LRO phases of the low- d LR-Heisenberg model, which is closely associated with GFFs, we introduce an LR-SRW (Levy flight) [44, 45] and impose the constraint that the total length \mathcal{L} is fixed at $\mathcal{L} \sim L^d$ (L denotes the linear system size), referred to as the fixed- \mathcal{L} LR-SRW. The length constraint reflects the extensivity of statistical systems. We obtain a key numerical observation that the two-point correlation function $g(r, L)$ of the fixed- \mathcal{L} LR-SRW behaves as

$$g(r, L) \sim \begin{cases} r^{2-d} \tilde{g}(r/L), & \sigma > 2, \\ \frac{r^{2-d}}{\ln r} \tilde{g}(r/L), & \sigma = 2, \\ r^{\sigma-d} \tilde{g}(r/L), & \sigma < 2. \end{cases} \quad (1)$$

For $d = 2$ and $\sigma > 2$, $g(r) \sim r^{2-d}$ does not decay as the two points are separated farther and farther away, leading to the well-known prediction for the absence of finite- T LRO in systems with continuous symmetry. For $d = 2$ and $\sigma = 2$, however, the logarithmic decay in Eq. (1), $g(r) \sim 1/\ln(r)$, gives an insightful indication that LRO could survive at finite- T , deviating from the prediction of the extended M-W theorem, which essentially relies on the GFF description. Since the magnitudes of GFFs exhibit logarithmic divergence, violating the extensivity of statistical systems, we suggest that the prediction of Eq. (1) could be more reliable.

We conduct a comparison study by performing extensive simulations of the fixed- \mathcal{L} LR-SRW and low- T LR-Heisenberg models in 2D and 3D. The results show that both systems display the same FSS behaviors for $\sigma \leq 2$ and $d = 2$, as well as for any $\sigma > 0$ and $d = 3$. In particular, the logarithmic scaling behaviors at $\sigma = 2$ for both $d = 2$ and 3, as predicted by Eq. (1), are clearly observed in the low- T LR-XY and LR-Heisenberg models, giving a strong indication that $\sigma^* = 2$ holds true for $d \geq 2$.

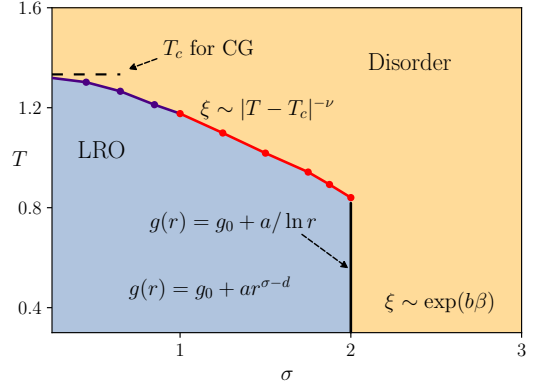


FIG. 1. The Phase diagram of the 2D LR-Heisenberg model, which includes: mean-field regime for $\sigma \leq 1$ with critical behaviors governed by the Gaussian fixed point, nonclassical regime for $1 < \sigma \leq 2$ with σ -dependent critical exponents, and SR regime for $\sigma > 2$ with neither LRO nor phase transition for $T > 0$. The correlation function $g(r)$ in the LRO phase behaves as $\sim g_0 + ar^{2-d-\eta_\ell}$ for $\sigma < 2$, with $\eta_\ell = 2 - \sigma$, and decays logarithmically as $\sim g_0 + a/\ln(r/r_0)$ for $\sigma = 2$. For $\sigma > 2$, the correlation length diverges as $\xi \sim \exp(b\beta)$, with b being a non-universal constant.

Based on whether or not the correlation function $g(r)$ would vanish in Eq. (1), we propose a criterion for determining the existence of finite- T LRO for systems with continuous symmetry: For $d < 2$, LRO can exist when $\sigma < \sigma_* = d$; For $d = 2$, LRO persists when $\sigma \leq \sigma_* = 2$; For $d > 2$, LRO always persists, but the system is not in the SR universality when $\sigma \leq \sigma_* = 2$.

Long-range Heisenberg model– We consider the LR-Heisenberg model on a square lattice with linear size L , described by Hamiltonian $\mathcal{H} = -\sum_{i<j} J/r_{i,j}^{d+\sigma} \mathbf{S}_i \cdot \mathbf{S}_j$, where \mathbf{S}_i and \mathbf{S}_j are 3-component classical unit spin vectors at sites i and j . Periodic boundary conditions are employed and the interaction strength J is normalized to satisfy: $\sum_{j>0} J/r_{0,j}^{2+\sigma} = 4$. Our simulation employs an enhanced version of the Luijten-Blöte (LB) algorithm [46, 47], which significantly accelerates the construction of clusters, and reduces the computational complexity, enabling simulation up to $L = 8192$ (see Ref. [39] for details). During the simulation, for a given configuration, we sample the squared magnetization $M^2 = |L^{-d} \sum_i \mathbf{S}_i|^2$ and the spin Fourier transform mode $M_k^2 = |L^{-d} \sum_i \mathbf{S}_i e^{i\mathbf{k} \cdot \mathbf{r}_i}|^2$, with $\mathbf{k} = (2\pi/L, 0)$ the smallest wave vector along the x-axis. We obtain: (1) the susceptibility $\chi = L^d \langle M^2 \rangle$; (2) the Fourier-transformed susceptibility $\chi_k = L^d \langle M_k^2 \rangle$; (3) the second-moment correlation length $\xi = 1/[2 \sin(|\mathbf{k}|/2)] \sqrt{\chi/\chi_k - 1}$, where $\langle \cdot \rangle$ denotes statistical average. For later convenience, we also introduce a rescaled quantity $D_k = L^2/\chi_k$.

Figure 2(a) compares the L -dependence of pseudo-critical inverse temperatures β_L , determined by the condition $\xi(\beta_L)/L = 1$, for $\sigma = 2$ and the nearest-neighbor

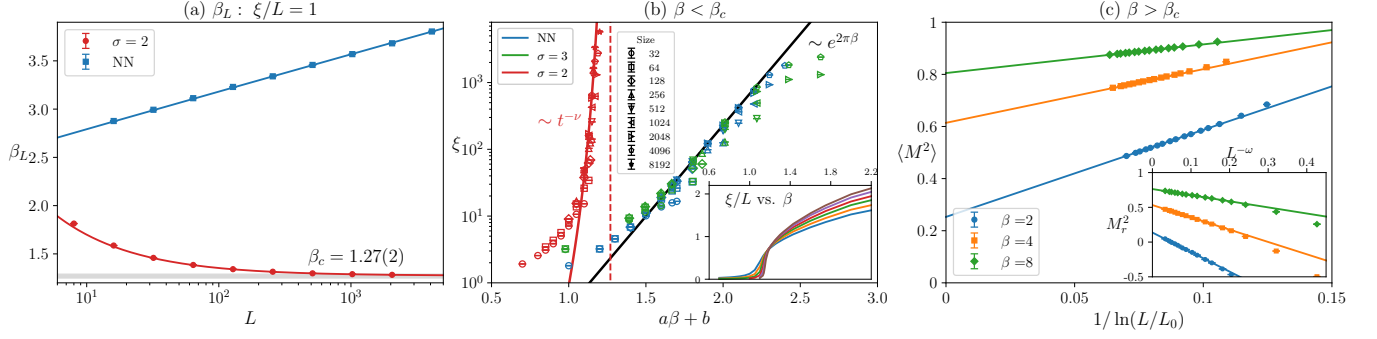


FIG. 2. Existence of the finite-T phase transition and emergence of LRO for the LR-Heisenberg model with $\sigma = 2$. (a) Semi-log plot of pseudo-critical points β_L versus L , determined by $\xi/L = 1$. For the NN case ($\sigma \rightarrow \infty$), β_L diverges logarithmically as $\beta_L \simeq (1/2\pi) \ln L$. For $\sigma = 2$, however, β_L decreases and rapidly converges as $\beta_L = \beta_c + bL^{-\omega}$ with $\beta_c = 1.27(2)$ and $\omega \approx 0.73$ (blue curve). (b) Different scaling behaviors of the correlation length ξ for $\sigma = 2$ and for $\sigma > 2$. Data points for different system sizes are marked by different symbols. For $\sigma > 2$, ξ remains finite for any $T > 0$, and, as $T \rightarrow 0$, it diverges as $\sim \exp(a\beta + b)$, where constants (a, b) are $(2\pi, 0)$ for the NN case and $(2.07, -1.09)$ for $\sigma = 3$ in the plot. For $\sigma = 2$, ξ diverges as $\sim (\beta_c - \beta)^{-\nu}$ with $\nu \approx 8$, where $\beta_c \approx 1.27$ can be roughly located in the inset. The inset plots ξ/L versus β for various L ranging from 64 to 2048 in a doubling sequence, where the approximately common intersection can be observed. (c) The LRO at $\beta = 2, 4, 8$ for $\sigma = 2$. The main plot demonstrates that the squared magnetization $\langle M^2 \rangle$ converges to positive values: 0.25, 0.61, 0.81, respectively, following a logarithmic decay: $\sim 1/\ln(L/L_0)$. The inset further displays the residual squared magnetization $M_r^2 = \langle M^2 \rangle - b\langle M_k^2 \rangle$, where the constant $b > 0$ is taken so that $M^2 > M_r^2$ for any finite L . With $b \approx 153, 182$, and 182 respectively, M_r^2 converge to non-vanishing values with corrections scaling as $L^{-\omega} \approx L^{-0.41}$, further showing the emergence of LRO for $L \rightarrow \infty$.

(NN) case ($\sigma \rightarrow \infty$), where β_L is plotted versus L (in log scale). As L increases, β_L for $\sigma = 2$ decreases and converges to $\beta_c = 1.27(2)$ with a power-law correction $\sim L^{-0.73}$, clearly showing the existence of a finite-T transition. In dramatic contrast, for the NN case, β_L diverges logarithmically as $\beta_L \propto (1/2\pi) \ln L$ [48], a hallmark of asymptotic freedom at low-T.

Figure 2(b) presents how the correlation length ξ grows as temperature decreases. Since ξ is inevitably restricted to $O(L)$ in a finite system, we progressively enlarge the simulated system size, as β increases, to keep track of the growth scaling of ξ in the thermodynamic limit ($L \rightarrow \infty$). For the NN case, ξ is finite for any finite-T and behaves asymptotically as $\sim e^{2\pi\beta}$ [48–51]; for $\sigma = 3$, by rescaling $\beta \rightarrow a\beta + b$ with $a = 2.07$ and $b = -1.09$, a nice data collapse with the NN case is achieved, demonstrating that the Heisenberg systems with $\sigma > 2$ are in the SR universality class and exhibit asymptotic freedom. For $\sigma = 2$, however, the data points display a clear bending-up in the semi-log plot, suggesting a scaling behavior that is qualitatively different from the SR case. A power-law scaling $\xi \sim t^{-\nu}$, characteristic of a second-order transition, is observed, with $t \equiv \beta_c - \beta$ and $\nu \approx 8$. Further, $\beta_c = 1.27$ can already be roughly identified from a bare-eye view of the inset, where the ratio ξ/L for different sizes exhibits an approximately common intersection.

Figure 2(c) presents the L -dependence of the squared magnetization $\langle M^2 \rangle$ for $\sigma = 2$ at different low temperatures. As L increases, $\langle M^2 \rangle$ clearly converges to a positive value following a logarithmic decay $\sim 1/\ln(L/L_0)$. The order parameter, $M \equiv \sqrt{\langle M^2 \rangle}$, reaches about 0.51,

0.78, 0.90 respectively for $\beta = 2, 4, 8$, demonstrating the emergence of LRO across the whole low-T phase with $\beta > \beta_c$. To further probe LRO with reduced finite-size effects, we define the residual squared magnetization $M_r^2 \equiv \langle M^2 \rangle - b\langle M_k^2 \rangle$ with $b > 0$ a positive constant. Since $\langle M_k^2 \rangle$ shares the same FSS behavior as the leading correction term in $\langle M^2 \rangle$, an appropriate choice of b effectively suppresses these corrections in M_r^2 . The inset shows that, at all the low temperatures, M_r^2 converges monotonically to a positive value that is consistent with that directly from $\langle M^2 \rangle$. Given the systematically increasing trend and the positivity at the largest accessible system sizes, it is highly unlikely that M_r^2 would vanish in the $L \rightarrow \infty$ limit. Further, since $b > 0$, M_r^2 serves as a lower bound for M^2 , confirming the existence of LRO.

Goldstone-mode physics and LR-SRW— We obtain strong numerical evidence that, as temperature decreases, the LR-Heisenberg model with $\sigma \leq 2$ exhibits spontaneous symmetry breaking and develops an LRO, via a single continuous phase transition (data for $\sigma < 2$ are given in Supplementary Materials (SM)). In the low-T LRO phase, the breaking of continuous symmetry is accompanied by the excitation of Goldstone modes (transverse fluctuations), which can be explored through the behavior of χ_k since it captures the distance-dependent part of the spin-spin correlation function. Figure 3(a) plots $D_k = L^2/\chi_k$ versus L (in the log-scale) for $\beta = 4$. The data points for both $\sigma = 1.75$ and 1.875 are well described by power-law divergence $\sim L^{2-\sigma}$ (the curves are from the fits $D_k = L^{2-\sigma}(a_0 + a_1 L^{-\omega})$), giving $\chi_k \sim L^\sigma$. This scaling behavior can be readily derived from the de-

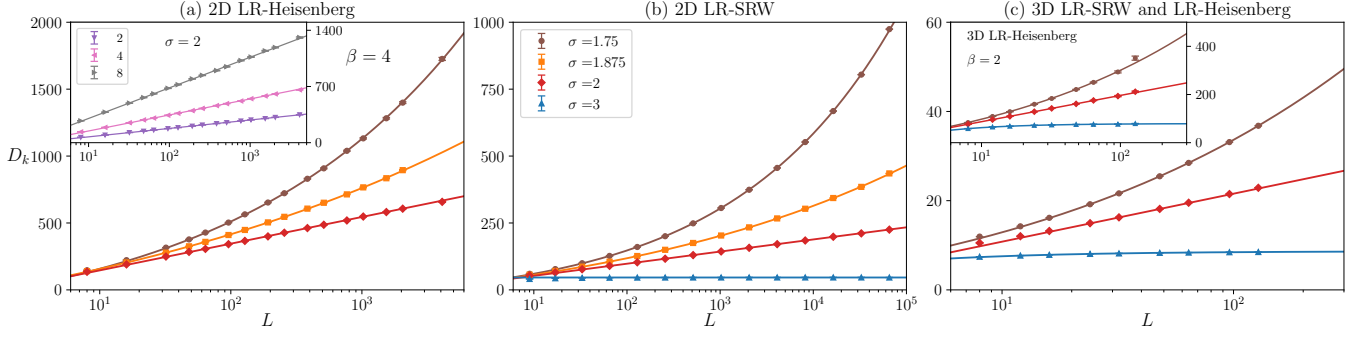


FIG. 3. The faithful characterization of the Goldstone-mode physics in the 2D and 3D LR-Heisenberg models at low-T by the fixed- \mathcal{L} LR-SRW. The rescaled quantity $D_k = L^2/\chi_k$ is plotted versus L (in log scale), for (a) the 2D LR-Heisenberg model, (b) the 2D fixed- \mathcal{L} LR-SRW, (c) the 3D fixed- \mathcal{L} LR-SRW, and (inset of (c)) the 3D LR-Heisenberg model; the inset of panel (a) is for $\sigma = 2$ at different low temperatures. In all cases, D_k follows a power law as $D_k \sim L^{2-\sigma}$ for $\sigma < 2$, and scales logarithmically as $D_k \sim \ln L$ for $\sigma = 2$. For $\sigma > 2$, both the 3D LR-Heisenberg and fixed- \mathcal{L} LR-SRW models have $\chi_k \sim L^2$.

scription of GFFs in the continuum limit (see the SM for details). For $\sigma = 2$, the linearity of data points shows a logarithmic scaling $\chi_k \sim L^2/\ln(L/L_0)$, which holds true at different low temperatures (inset of Fig. 3(a)). Unfortunately, this logarithmic scaling of χ_k can no longer be derived from GFFs, where the logarithmically diverging magnitude of fields makes the situation very subtle.

Inspired by the fact that simple random walk (SRW) plays a vital role in describing and proving the critical behaviors of $O(n)$ spin models in high dimensions, we introduce a LR-SRW model (Levy flight) with the total length \mathcal{L} fixed at $O(L^d)$, which we call fixed- \mathcal{L} LR-SRW. The fixed-length constraint reflects the extensivity of statistical systems and avoids the amplitude divergence of the GFFs for $\sigma \geq 2$. Periodic simple cubes of linear size L are considered, and the length \mathcal{L} is fixed at $L^2/4$ and L^3 for 2D and 3D, respectively. The LR interaction is realized by r -dependent transition probability $p(\mathbf{r}) \sim 1/r^{d+\sigma}$. Given a LR-SRW configuration, a height field $h(\mathbf{x})$ is recorded to account for the number of visited times at site \mathbf{x} , and a Fourier “magnetization density” is obtained as $M_k = (1/L^d) \sum h(\mathbf{x})e^{i\mathbf{k}\cdot\mathbf{x}}$, where $\mathbf{k} = (2\pi/L, 0)$. The corresponding “susceptibility” $\chi_k = L^d \langle M_k^2 \rangle$ and the rescaled quantity $D_k = L^2/\chi_k$ are then calculated.

A comparison of Figs. 3(a) and (b) clearly suggests that, in 2D and for $\sigma \leq 2$, the low-T LR-Heisenberg and the fixed- \mathcal{L} LR-SRW systems display the same scaling behaviors of D_k : $\sim \ln L$ for $\sigma = 2$ and $\sim L^{2-\sigma}$ for $\sigma = 1.875$ and 1.75 . For $\sigma > 2$, no such equivalence holds, since no LRO emerges in the LR-Heisenberg model.

Figure 3(c) further demonstrates the equivalence in 3D. For the LR-Heisenberg model, the simulation at $\beta = 2$ is deeply in the LRO phase, since the critical temperature is $\beta_c \approx 0.693$ for the NN case [52] and increases as σ decreases. Again, the two dramatically different systems, the LR-SRW and LR-Heisenberg models, display the same scaling behaviors of D_k : $\sim L^{2-\sigma}$ for $\sigma < 2$,

$\sim \ln L$ for $\sigma = 2$, and $\sim L^0$ for $\sigma > 2$.

In short, Figs. 3(a-c) show that the fixed- \mathcal{L} LR-SRW can correctly capture the Goldstone-mode physics in the LRO phase of LR spin systems with continuous symmetries. Particularly, for $\sigma = 2$, the logarithmic scaling behaviors $\chi_k \sim L^2/\ln(L/L_0)$ are observed in both 2D and 3D, which can hardly be attributed to finite-size corrections. These low-T properties strongly suggest that the LR-Heisenberg model has $\sigma^* = 2$, separating the SR and the nonclassical regimes.

Proposal of a general criterion— The FSS of χ_k in Figs. 3(a-c) indicates that the two-point *connected* correlation function, $g(\mathbf{r}, L) \equiv \langle \delta(\mathbf{0}) \cdot \delta(\mathbf{r}) \rangle$, admits a universal expression as Eq. (1), with $\delta(\mathbf{r}) = h(\mathbf{r}) - \langle h \rangle$ for LR-SRW and $\delta(\mathbf{r}) = \mathbf{S}(\mathbf{r}) - \langle \mathbf{S} \rangle$ for LR-spin systems at low-T, which is further numerically confirmed by simulating the fixed- \mathcal{L} LR-SRW and analyzing $g(\mathbf{r}, L)$ in 2D and 3D (see SM for details).

We can then infer from Eq. (1) under what conditions the Goldstone-mode fluctuations would destroy the LRO in $O(n)$ spin systems with $n \geq 2$. For $d < 2$ and $\sigma \geq d$, the correlation function $g(r)$ remains as a finite constant or diverges as distance r increases, indicating that the contribution of Goldstone modes to $g(r)$ is significant and can disrupt the LRO; the same occurs for $d = 2$ and $\sigma > 2$. A special case is for $(d, \sigma) = (2, 2)$, where $g(r)$ vanishes logarithmically and the LRO can emerge at low-T. For $d > 2$, the system always exhibits the LRO, but the low-T Goldstone-mode physics for $\sigma \leq 2$ differs from that for $\sigma > 2$. On this basis, we propose the following general criterion for the $O(n)$ spin systems with $n \geq 2$:

- For $d < 2$, when $\sigma < \sigma_* = 2$, the system resides in the nonclassical regime and exhibits the LRO.
- For $d = 2$, when $\sigma \leq \sigma_* = 2$, the system resides in the nonclassical regime and exhibits the LRO.
- For $d > 2$, the system resides in the nonclassical

regime when $\sigma \leq \sigma_* = 2$, while maintaining the LRO across all values of σ .

Discussion and outlook— We conduct large-scale simulations of the 2D LR-Heisenberg model, and show that for $\sigma \leq 2$, it undergoes a second-order phase transition at $\beta_c = 1.27$ and develops the LRO for $\beta > \beta_c$, consistent with the recent results for the 2D LR-XY model [39, 40]. We then introduce the fixed- \mathcal{L} LR-SRW model and find that it can faithfully capture Goldstone-mode physics in the LRO phase for $\sigma \leq 2$ in 2D and for any $\sigma > 0$ in 3D, including, in particular, the logarithmic scaling at $\sigma = 2$. Finally, we conjecture Eq. (1) for the connected correlation function in the LRO, and numerically confirm it for the fixed- \mathcal{L} LR-SRW in 2D and 3D. On this basis, we propose a criterion in the (d, σ) plane, which can predict the emergence of the LRO and the nature of phase transitions for LR systems with continuous symmetry.

To examine how general the proposed criterion is, we further study the 2D LR uniform forest (UF) model (see SM), which is a correlated bond-percolation model with the constraint that no cycles exist. Despite involving no spins, the LR-UF model can be formulated as a nonlinear sigma model with target space being the supersphere $\mathbb{H}^{0|2}$, and thus possesses a continuous supersymmetry [53, 54]. Interestingly, the 2D LR-UF and LR-Heisenberg models behave analogously: they develop the LRO via a continuous transition for $\sigma \leq 2$, and exhibit asymptotic freedom for $\sigma > 2$. This provides another concrete example supporting our general criterion.

For $\sigma = 2$, while conflicting with the extended M-W theorem that is essentially based on the logarithmic divergence of GFFs, the emergence of the LRO in low-T LR systems is well consistent with the fixed- \mathcal{L} LR-SRW. We note that, for $\sigma > 2$ in 2D, both the GFF and the fixed- \mathcal{L} LR-SRW description fail to correctly capture the low-T physics in the LR-XY and LR-Heisenberg models, although they can predict the absence of LRO. Specifically, the XY model is effectively described by the sine-Gordon model [55, 56] and the Heisenberg model is described by the nonlinear sigma model [57, 58]. Therefore, we argue that the GFF description fails at the subtle case of $\sigma = 2$, and that an appropriate treatment of the LR sine-Gordon and the nonlinear sigma models is most probably needed. Finally, it is also desired to reexamine the field theoretical description of LR- $O(n)$ spin models and the associated RG calculations.

YD is indebted to Lode Pollet for valuable discussions. We acknowledge the support from the National Natural Science Foundation of China (NSFC) under Grant No. 12204173 and No. 12275263, as well as the Innovation Program for Quantum Science and Technology (under Grant No. 2021ZD0301900). YD is also supported by the Natural Science Foundation of Fujian Province 802 of China (Grant No. 2023J02032).

* These two authors contributed equally to this work

† zfanac@ustc.edu.cn

‡ yjdeng@ustc.edu.cn

- [1] K. von Klitzing, Rev. Mod. Phys. **58**, 519 (1986).
- [2] D. C. Tsui, H. L. Stormer, and A. C. Gossard, Phys. Rev. Lett. **48**, 1559 (1982).
- [3] C. Cui-Zu, Z. Jinsong, F. Xiao, S. Jie, Z. Zuocheng, G. Minghua, L. Kang, O. Yunbo, W. Pang, W. Li-Li, J. Zhong-Qing, F. Yang, J. Shuaihua, C. Xi, J. Jinfeng, D. Xi, F. Zhong, Z. Shou-Cheng, H. Ke, W. Yayu, L. Li, M. Xu-Cun, and X. Qi-Kun, Science **340**, 167 (2013).
- [4] C. L. Kane and E. J. Mele, Phys. Rev. Lett. **95**, 226801 (2005).
- [5] B. B. Andrei, H. Taylor L., and Z. Shou-Cheng, Science **314**, 1757 (2006).
- [6] K. Markus, W. Steffen, B. Christoph, R. Andreas, B. Hartmut, M. Laurens W., Q. Xiao-Liang, and Z. Shou-Cheng, Science **318**, 766 (2007).
- [7] N. D. Mermin and H. Wagner, Phys. Rev. Lett. **17**, 1133 (1966).
- [8] J. M. Kosterlitz, Rev. Mod. Phys. **89**, 040501 (2017).
- [9] F. J. Dyson, Communications in Mathematical Physics **12**, 91 (1969).
- [10] S. Maleev, Soviet Journal of Experimental and Theoretical Physics **43**, 1240 (1976).
- [11] J. Fröhlich, R. Israel, E. H. Lieb, and B. Simon, Communications in Mathematical Physics **62**, 1 (1978).
- [12] N. Defenu, T. Donner, T. Macrì, G. Pagano, S. Ruffo, and A. Trombettoni, Rev. Mod. Phys. **95**, 035002 (2023).
- [13] M. E. Fisher, S.-k. Ma, and B. G. Nickel, Phys. Rev. Lett. **29**, 917 (1972).
- [14] J. Sak, Physical Review B **8**, 281 (1973).
- [15] J. Honkonen and M. Y. Nalimov, J. Phys. A: Math. Theor. **22**, 751 (1989).
- [16] J. Honkonen, J. Phys. A: Math. Theor. **23**, 825 (1990).
- [17] N. Defenu, A. Trombettoni, and A. Codello, Phys. Rev. E **92**, 052113 (2015).
- [18] E. Luijten and H. W. J. Blöte, Phys. Rev. Lett. **89**, 025703 (2002).
- [19] M. C. Angelini, G. Parisi, and F. Ricci-Tersenghi, Phys. Rev. E **89**, 062120 (2014).
- [20] T. Horita, H. Suwa, and S. Todo, Physical Review E **95**, 012143 (2017).
- [21] S. Shiratani and S. Todo, Phys. Rev. E **110**, 064106 (2024).
- [22] M. Picco, Critical behavior of the Ising model with long range interactions (2012), arXiv:1207.1018 [cond-mat, physics:hep-th].
- [23] T. Blanchard, M. Picco, and M. A. Rajabpour, Europhys. Lett. **101**, 56003 (2013).
- [24] P. Grassberger, J. Stat. Phys. **153**, 289 (2013).
- [25] P. Bruno, Physical Review Letters **87**, 137203 (2001).
- [26] N. Laflorencie, I. Affleck, and M. Berciu, Journal of Statistical Mechanics: Theory and Experiment **2005**, P12001 (2005).
- [27] M. F. Maghrebi, Z.-X. Gong, and A. V. Gorshkov, Phys. Rev. Lett. **119**, 023001 (2017).
- [28] R.-G. Zhu and A.-M. Wang, Phys. Rev. B **74**, 012406 (2006).
- [29] A. Cavallo, F. Cosenza, and L. De Cesare, Phys. Rev. B **66**, 174439 (2002).

- [30] E. Yusuf, A. Joshi, and K. Yang, Phys. Rev. B **69**, 144412 (2004).
- [31] A. Cavallo, F. Cosenza, and L. De Cesare, Physica A: Statistical Mechanics and its Applications **332**, 301 (2004).
- [32] F. Cescatti, M. Ibáñez Berganza, A. Vezzani, and R. Burioni, Phys. Rev. B **100**, 054203 (2019).
- [33] J. R. de Sousa, The European Physical Journal B - Condensed Matter and Complex Systems **43**, 93 (2005).
- [34] B. Sbierski, M. Bintz, S. Chatterjee, M. Schuler, N. Y. Yao, and L. Pollet, Phys. Rev. B **109**, 144411 (2024).
- [35] J. Zhao, M. Song, Y. Qi, J. Rong, and Z. Y. Meng, npj Quantum Materials **8**, 59 (2023).
- [36] A. Tiwari, H. Ahn, B. Kumar, J. Saini, P. K. Srivastava, B. Singh, C. Lee, and S. Ghosh, Phys. Rev. B **109**, L020407 (2024).
- [37] G. Giachetti, N. Defenu, S. Ruffo, and A. Trombettoni, Phys. Rev. Lett. **127**, 156801 (2021).
- [38] G. Giachetti, A. Trombettoni, S. Ruffo, and N. Defenu, Phys. Rev. B **106**, 014106 (2022).
- [39] D. Yao, T. Xiao, C. Zhang, Y. Deng, and Z. Fan, Phys. Rev. B **112**, 144429 (2025).
- [40] T. Xiao, D. Yao, C. Zhang, Z. Fan, and Y. Deng, Chinese Physics Letters **42**, 070002 (2025).
- [41] Z. Zhou, J. Grimm, S. Fang, Y. Deng, and T. M. Garoni, Phys. Rev. Lett. **121**, 185701 (2018).
- [42] Y. Deng, T. M. Garoni, J. Grimm, and Z. Zhou, Journal of Statistical Mechanics: Theory and Experiment **2022**, 053208 (2022).
- [43] Y. Deng, T. M. Garoni, J. Grimm, and Z. Zhou, Journal of Statistical Mechanics: Theory and Experiment **2024**, 023203 (2024).
- [44] J.-P. Bouchaud and A. Georges, Physics reports **195**, 127 (1990).
- [45] V. Zaburdaev, S. Denisov, and J. Klafter, Rev. Mod. Phys. **87**, 483 (2015).
- [46] E. Luijten and H. W. Blöte, International Journal of Modern Physics C (IJMPC) **06**, 359 (1995).
- [47] E. Luijten and H. W. J. Blöte, Physical Review B **56**, 8945 (1997).
- [48] D. Yao, C. Zhang, Z. Y. Xie, Z. Fan, and Y. Deng, Phys. Rev. B **111**, 214403 (2025).
- [49] S. Caracciolo and A. Pelissetto, Nuclear Physics B **420**, 141 (1994).
- [50] M. Falcioni and A. Treves, Nuclear Physics B **265**, 671 (1986).
- [51] A. Billoire, Phys. Rev. B **54**, 990 (1996).
- [52] Y. Sun, M. Hu, Y. Deng, and J.-P. Lv, Phys. Rev. Lett. **131**, 207101 (2023).
- [53] H. Chen, J. Salas, and Y. Deng, SciPost Phys. **16**, 121 (2024).
- [54] R. Bauerschmidt, N. Crawford, T. Helmuth, and A. Swan, Communications in Mathematical Physics **381**, 1223 (2021).
- [55] J. José, Phys. Rev. D **14**, 2826 (1976).
- [56] J. Fröhlich, Communications in Mathematical Physics **47**, 233 (1976).
- [57] E. Brézin and J. Zinn-Justin, Phys. Rev. Lett. **36**, 691 (1976).
- [58] A. Polyakov, Physics Letters B **59**, 79 (1975).

Supplemental Material for “Spontaneous Symmetry Breaking in Two-dimensional Long-range Heisenberg Model”

2D LR-HEISENBERG MODEL AT $\sigma \leq 2$

In this section, we present supplemental results on the critical properties and low-temperature (low-T) behavior of the 2D long-range (LR) Heisenberg model for $\sigma \leq 2$ (specifically, at $\sigma = 1.75, 1.875$, and 2). As discussed in the main text, these systems undergo a finite-temperature second-order phase transition to a long-range-ordered phase.

Figure S1 displays the critical characteristics for $\sigma = 1.75, 1.875$, and 2 . The main panels show ξ/L as a function of the inverse temperature β . In all cases, the pronounced crossing of curves for different system sizes L signifies a second-order transition. The insets illustrate the finite-size scaling (FSS) of the pseudo-critical inverse temperature β_L —determined by fixing ξ/L near its critical value as a function of L . For each σ , β_L converges toward the thermodynamic critical point following a power-law decay $\beta_L - \beta_c \sim L^{-\omega}$, further confirming the existence of a finite-T phase transition. Specific parameter values are shown in Fig. S1.

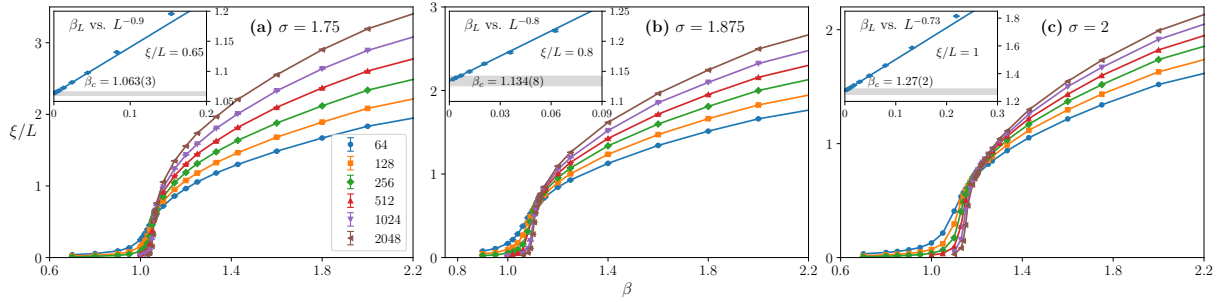


FIG. S1. Demonstration of the second-order phase transition for $\sigma = 1.75$ (a), 1.875 (b) and 2 (c). Main plots display the second-order correlation length ratio (to the system size) ξ/L as a function of the inverse temperature β . The clear crossing behavior among curves with different L signifies the existence of a second-order phase transition. The insets illustrate pseudo-critical point β_L when ξ/L is fixed at $0.65, 0.8$ and 1 for $\sigma = 1.75, 1.875$ and 2 . In all cases, β_L exhibits power-law convergence to a finite critical point.

Figure S2 demonstrates the presence of long-range order (LRO) at low temperatures for $\sigma \leq 2$. Panels (a1), (b1), and (c1) show the L dependence of the squared magnetization $\langle M^2 \rangle$. As discussed in the main text, Goldstone mode analysis predicts that spatial correlations decay as $\sim r^{\sigma-d}$ for $\sigma < 2$ and $\sim r^{2-d}/\ln r$ for $\sigma = 2$. Consequently, in the LRO phase, the finite-size scaling of $\langle M^2 \rangle$ is expected to follow:

$$\langle M^2 \rangle = c_1 + c_2 L^{\sigma-2} \quad \text{for } \sigma < 2, \quad (\text{S1})$$

$$\langle M^2 \rangle = c_1 + c_2 / \ln(L/L_0) \quad \text{for } \sigma = 2, \quad (\text{S2})$$

where c_1, c_2 represent different constants. Accordingly, panels (a1) and (b1) plot $\langle M^2 \rangle$ as a function of $L^{\sigma-2}$ for $\sigma = 1.75$ and 1.875 , respectively, while panel (c1) plots $\langle M^2 \rangle$ versus $1/\ln(L/L_0)$ for $\sigma = 2$. In all cases, the data exhibit linear scaling with a finite positive intercept as $L \rightarrow \infty$, confirming spontaneous magnetization.

To mitigate finite-size effects, we analyze the rescaled magnetization defined as $M_r^2 = \langle M^2 \rangle - b \langle M_k^2 \rangle$ with $b > 0$, which eliminates the leading-order correction in $\langle M^2 \rangle$. As shown in Panels (a2), (b2), and (c2), M_r^2 converges to a positive value via power-law scaling with increasing L for all cases. Furthermore, given the monotonic increase of M_r^2 with L and the already positive values observed at the largest simulated system size, M_r^2 is unlikely to reduce to 0 in the thermodynamic limit $L \rightarrow \infty$. Since M_r^2 serves as a lower bound of the magnetization $\langle M^2 \rangle$, this result further confirms the existence of LRO at low temperatures for $\sigma \leq 2$.

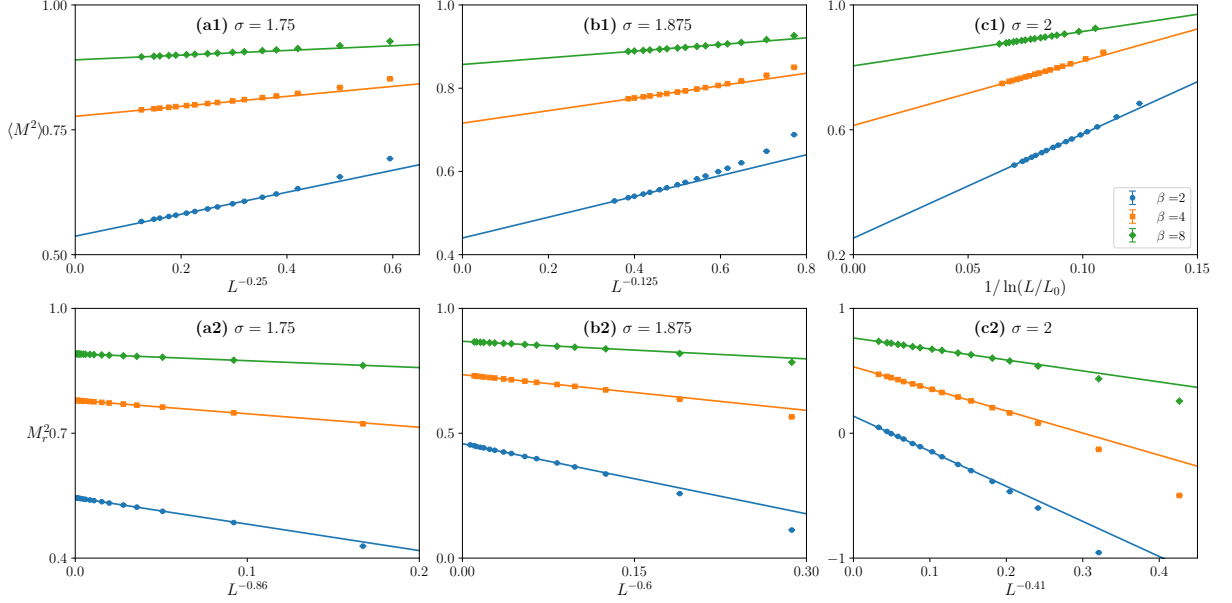


FIG. S2. Demonstration of LRO for $\sigma = 1.75, 1.875$ and 2 . The upper figures display the L -dependence of the magnetization $\langle M^2 \rangle$. For $\sigma = 1.75$ (a1) and 1.875 (b1), $\langle M^2 \rangle$ converges to positive values as $\sim L^{\sigma-2}$; for $\sigma = 2$ (c1), $\langle M^2 \rangle$ converges logarithmically to positive values with $L_0 = e^{-5.94}, e^{-7.1}, e^{-7.4}$ for $\beta = 2, 4, 8$. The lower figures displays the rescaled magnetization $M_r^2 = \langle M^2 \rangle - b\langle M_k^2 \rangle$ with $b = 19, 40$ for $\sigma = 1.75$ (a2), 1.875 (b2) and $b = 152, 182, 182$ for $\beta = 2, 4, 8$ in $\sigma = 2$ (c2). In all cases, M_r^2 exhibits suppressed finite-size corrections and converges to a positive value in the $L \rightarrow \infty$ limit.

GAUSSIAN FREE FIELD DESCRIPTION FOR GOLDSTONE MODE

The effective Hamiltonian of the LR- $O(n)$ spin model in momentum space is given by [1]:

$$\begin{aligned} \beta H = & \int \frac{d^d q}{(2\pi)^d} \left(\frac{t}{2} + \frac{K_2}{2} q^2 + K_\sigma q^\sigma \right) \Psi(\mathbf{q}) \cdot \Psi(-\mathbf{q}) + \\ & \int \frac{d^d q_1}{(2\pi)^d} \int \frac{d^d q_2}{(2\pi)^d} \int \frac{d^d q_3}{(2\pi)^d} u \\ & \Psi(\mathbf{q}_1) \cdot \Psi(\mathbf{q}_2) \cdot \Psi(\mathbf{q}_3) \cdot \Psi(-\mathbf{q}_1 - \mathbf{q}_2 - \mathbf{q}_3), \end{aligned} \quad (\text{S3})$$

where \mathbf{q} denotes a d -dimensional momentum variable and $\Psi(\mathbf{q})$ is the Fourier transform of a locally defined n -component spin field $\Psi(\mathbf{x})$; t, K_2, K_σ , and u are interacting parameters, and t varies linearly with the distance to criticality.

As demonstrated in Fig. S2, the 2D LR-Heisenberg model with $\sigma \leq 2$ exhibits spontaneous symmetry breaking and Goldstone mode excitations at low temperatures. Upon spontaneous symmetry breaking, the field can be decomposed within a mean-field approximation into a finite longitudinal component $\bar{\Psi} = \sqrt{-t/(4u)}$ and small transverse fluctuations Ψ_T :

$$\Psi(\mathbf{x}) = \bar{\Psi} \hat{\mathbf{e}}_l + \Psi_T(\mathbf{x}) \hat{\mathbf{e}}_t, \quad (\text{S4})$$

where $\hat{\mathbf{e}}_l$ and $\hat{\mathbf{e}}_t$ represent the longitudinal and transverse direction vectors, respectively. Substituting Eq. (S4) into the Hamiltonian (S3) and retaining terms up to quadratic order yields the effective Hamiltonian for the transverse modes [2]:

$$\beta H = V \left(\frac{t}{2} \bar{\Psi}^2 + u \bar{\Psi}^4 \right) + \frac{1}{V} \sum_{\mathbf{q}} \left(K_\sigma q^\sigma + \frac{K_2}{2} q^2 \right) \cdot |\Psi_T(\mathbf{q})|^2, \quad (\text{S5})$$

where V denotes the volume of the system. Therefore, the Hamiltonian of the transverse modes corresponds to a Gaussian free field (GFF). For $\sigma < 2$, the long-range term $K_\sigma q^\sigma$ dominates the short-range q^2 term in the infrared limit ($q \rightarrow 0$). This leads to a power-law decay of the two-point correlation function: $g(r) \sim r^{\sigma-d}$. However, at

$\sigma = 2$, this GFF description breaks down due to the logarithmic infrared divergence of the transverse fluctuations, which would theoretically destroy the LRO. Nevertheless, numerical simulations demonstrate robust LRO at $\sigma = 2$, indicating that the simple GFF description is insufficient at the marginal point.

THE CORRELATION FUNCTION IN FIXED- \mathcal{L} LR-SRW

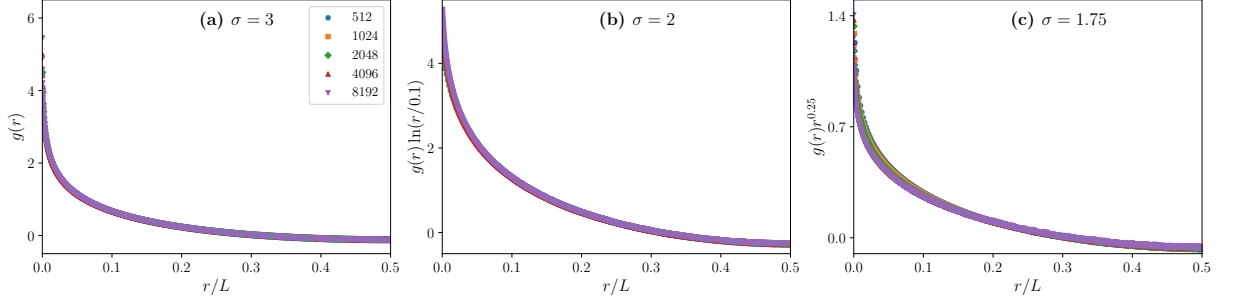


FIG. S3. FSS analysis of the correlation function for different σ in 2D fixed- \mathcal{L} LR-SRW. The rescaled correlations – specifically $g(r)$, $g(r) \ln(r/0.1)$, and $g(r)r^{0.25}$ for $\sigma = 3$ (a), 2 (b), and 1.75 (c), respectively – are plotted as a function of the scaled distance r/L . The excellent collapse of curves for different system sizes L confirms the validity of the conjectured scaling form in Eq. (S6).

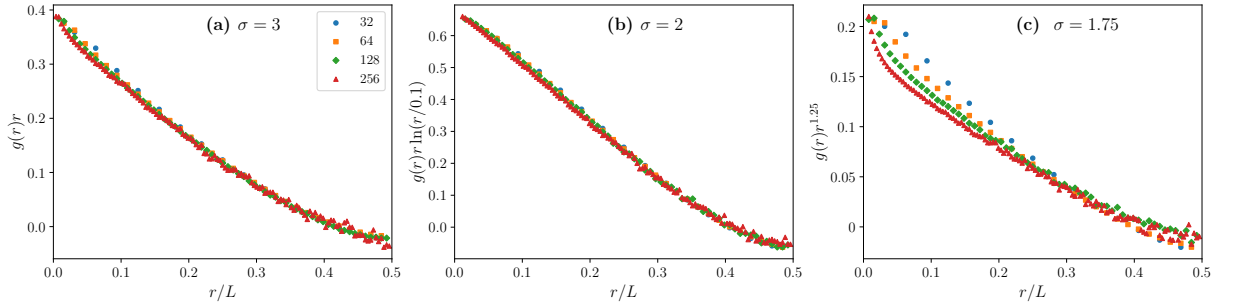


FIG. S4. FSS analysis of the correlation function for the 3D fixed- \mathcal{L} LR-SRW with different σ . Rescaled correlation functions – $g(r)r$, $g(r)r \ln(r/0.1)$, $g(r)r^{1.25}$ for $\sigma = 3$ (a), 2 (b) and 1.75 (c) respectively – is plotted as a function of r/L . For $\sigma = 3$ and 2, the data for different system sizes collapse well onto a universal curve. For $\sigma = 1.75$, the minor deviations are attributed to strong finite-size corrections. The overall collapse of the curves for different system sizes confirms the validity of the conjectured scaling form in Eq. (S6).

In this section, we employ FSS analysis to validate the conjectured correlation function of fixed- \mathcal{L} long-range simple random walk (LR-SRW):

$$g(\mathbf{r}, L) \sim \begin{cases} r^{2-d} & \tilde{g}(r/L), \quad \sigma > 2, \\ r^{2-d}/\ln r & \tilde{g}(r/L), \quad \sigma = 2, \\ r^{\sigma-d} & \tilde{g}(r/L), \quad \sigma < 2. \end{cases} \quad (\text{S6})$$

According to Eq. (S6), the appropriately rescaled correlations are expected to collapse onto a single master curve $\tilde{g}(x)$ when plotted against the scaling variable $x = r/L$. Specifically, for $\sigma > 2$, the correlation function $g(r)$ is rescaled as $r^{d-2}g(r)$; for $\sigma = 2$, as $r^{d-2} \ln(r/r_0)g(r)$; and for $\sigma < 2$, as $r^{d-\sigma}g(r)$. Figures S3 and S4 display the rescaled correlation functions for $d = 2$ and $d = 3$, respectively, with $\sigma = 3, 2$ and 1.75. In the 2D case, data for all values of σ exhibit excellent collapse across different system sizes. For the 3D systems, the data collapse is robust for $\sigma = 3$ and 2. However, for $\sigma = 1.75$, minor deviations are observed in $\tilde{g}(r/L)$ among different system sizes. We attribute these deviations to strong finite-size corrections, as evidenced by the diminishing discrepancy with increasing L . It is expected that the collapse quality will further improve with larger system sizes. Overall, the consistent data collapse validates the conjectured scaling form given in Eq. (S6).

2D LR SPANNING FOREST AT THE BOUNDARY CASE $\sigma = 2$

In the main text, we concluded that two-dimensional (2D) spin systems with continuous symmetry, when endowed with LR interactions decaying as $\sim 1/r^{d+\sigma}$, undergo a second-order phase transition at $\sigma = 2$ and exhibit LRO at low temperatures. In this section, we extend our investigation to a 2D geometric model, which also possesses continuous symmetry – the uniform forest (UF) model.

The UF model is defined on a lattice where a configuration \mathcal{A} consists of a spanning forest (a collection of acyclic clusters). Each occupied bond is assigned a weight w . The partition function of the model can be written as:

$$Z = \sum_{\mathcal{A}} w^{|\mathcal{A}|} \delta_{c(\mathcal{A}),0}, \quad (\text{S7})$$

where the sum runs over all possible configurations \mathcal{A} , $|\mathcal{A}|$ denotes the total number of bonds of \mathcal{A} and the Kronecker delta $\delta_{c(\mathcal{A}),0}$ enforces the constraint of zero cyclomatic number $c(\mathcal{A})$ (i.e., no loops allowed). Field-theoretically, the UF model can be described as a nonlinear sigma model with the target space being the supersphere $\mathbb{H}^{0|2}$ [3, 4]. Renormalization group analyses indicate that for spatial dimension $d \geq 3$, the UF model exhibits spontaneous symmetry breaking of the $\mathbb{H}^{0|2}$ symmetry [5]. In the large- w regime (corresponding to the low-T phase), the two-point correlation function decays algebraically due to the Goldstone modes associated with continuous symmetry breaking. Analogous to the 2D Heisenberg model, the 2D short-range (SR) UF model lacks a finite-T phase transition and exhibits asymptotic freedom.

When LR interactions are introduced, bonds between arbitrarily distant sites i and j can be occupied with a weight $w/r_{ij}^{d+\sigma}$. The partition function of the resulting LR-UF model becomes:

$$Z = \sum_{\mathcal{A}} \prod_{(i,j)} \frac{w}{r_{ij}^{d+\sigma}} \delta_{c(\mathcal{A}),0}, \quad (\text{S8})$$

where the product runs over all bonds (i,j) occupied in configuration \mathcal{A} . Here, we study the phase transition and low-T behavior of the 2D LR-UF model at $\sigma = 2$. Our results demonstrate that this system also undergoes a second-order phase transition into an LRO phase at low temperatures. This result suggests that the conclusions drawn in the main text are not limited to spin systems but apply broadly to models with continuous symmetry, thereby significantly expanding the scope of our theoretical framework.

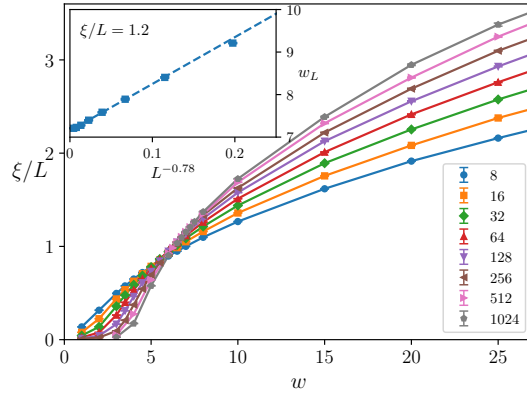


FIG. S5. Second-order phase transition in the 2D LR-UF model at $\sigma = 2$. The main panel plots the correlation length ratio ξ/L as a function of the weight w (analogous to the inverse temperature) for different system sizes L . The crossing of curves for different L s signifies a second-order phase transition near $w_c \approx 7$. The inset shows the FSS of the pseudo-critical point w_L , defined by the condition $\xi/L = 1.2$. The pseudo-critical point converges to the thermodynamic critical point $w_c \approx 7$ following a power law $\sim L^{-0.78}$.

To characterize the phase transition, we introduce observables based on auxiliary Ising spins. The configuration of the UF model consists of a set of clusters without loops. Analogous to the Fortuin-Kasteleyn (FK) representation of the spin model [6], for each cluster in the configuration, we assign a spin value chosen uniformly at random from $\{+1, -1\}$, and set s_i for all sites within that cluster to this value. Using the introduced spin variables, we then calculate the magnetization density $M^2 = L^{-4} |\sum_i s_i|^2$, spin Fourier transform mode $M_k^2 = L^{-4} |\sum_i s_i e^{i\mathbf{k} \cdot \mathbf{r}_i}|$, $\chi_k = L^2 \langle M_k^2 \rangle$ and second-moment correlation length $\xi = 1/[2 \sin(|\mathbf{k}|/2)] \sqrt{\langle M^2 \rangle / \langle M_k^2 \rangle - 1}$.

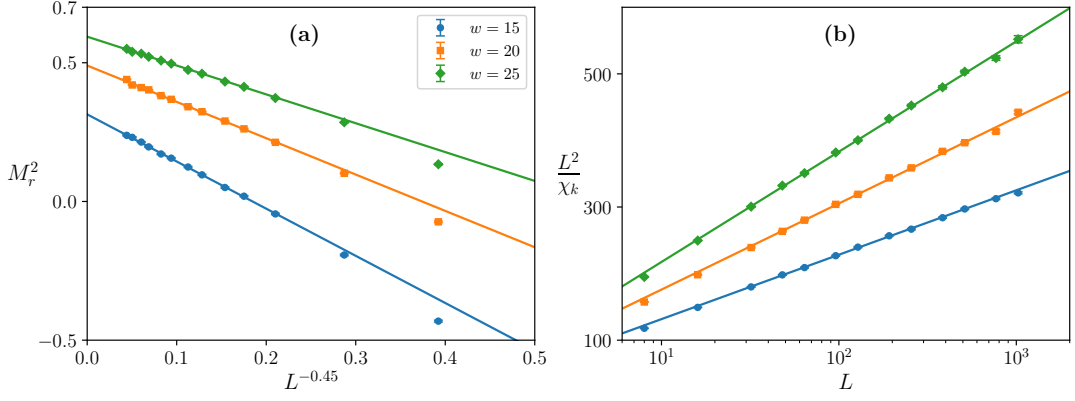


FIG. S6. Evidence of LRO and Goldstone modes in 2D LR-UF model at $\sigma = 2$ in the low-temperature phase ($w = 15, 20$, and 25 ; note that $w_c \approx 7$ from Fig. S5). (a) FSS of the rescaled magnetization $M_r^2 = \langle M^2 \rangle - b\langle M_k^2 \rangle$ with $b = 150$. For all w , M_r^2 converges to positive values scaling as $\sim L^{-0.45}$, confirming the existence of LRO. (b) The quantity L^2/χ_k is plotted against L on a semi-logarithmic scale. In all cases, the linear dependence implies $L^2/\chi_k \sim \ln L$, and hence $\chi_k \sim L^2/\ln(L/L_0)$.

Figures S5 and S6 present the critical and low-temperature properties of the LR-UF model at $\sigma = 2$. Fig. S5 displays ξ/L as a function of the bond weight w . The distinct crossing of curves for different system sizes signifies a second-order phase transition. By fixing ξ/L near its critical value, we analogously define the pseudo-critical point w_L . The inset shows the FSS of w_L with increasing L , which converges to a finite value following a power law $\sim L^{-\omega}$, with $\omega = 0.78$ obtained from data fitting, confirming the existence of a finite-T transition.

Figure S6 provides evidence for LRO and Goldstone modes at low temperatures. Panel (a) displays the FSS of the rescaled magnetization $M_r^2 = \langle M^2 \rangle - b\langle M_k^2 \rangle$ at different low temperatures. The convergence of M_r^2 to a positive value acts as a lower bound for $\langle M^2 \rangle$, confirming LRO across the low-T regime. Panel (b) illustrates that at low temperatures and for different w , the transverse susceptibility scales as $\chi_k \sim L^2/\ln(L/L_0)$. This logarithmic scaling is consistent with the presence of Goldstone modes in 2D systems with $\sigma = 2$, as in Fig. 3 in the main text.

-
- [1] M. E. Fisher, S.-k. Ma, and B. G. Nickel, Critical exponents for long-range interactions, *Phys. Rev. Lett.* **29**, 917 (1972).
 - [2] M. Kardar, *Statistical Physics of Fields* (Cambridge University Press, Cambridge, 2007).
 - [3] H. Chen, J. Salas, and Y. Deng, Anomalous criticality coexists with giant cluster in the uniform forest model, *SciPost Phys.* **16**, 121 (2024).
 - [4] R. Bauerschmidt, N. Crawford, T. Helmuth, and A. Swan, Random spanning forests and hyperbolic symmetry, *Communications in Mathematical Physics* **381**, 1223 (2021).
 - [5] R. Bauerschmidt, N. Crawford, and T. Helmuth, Percolation transition for random forests in $d \geq 3$, *Inventiones mathematicae* **237**, 445 (2024).
 - [6] P. Hou, S. Fang, J. Wang, H. Hu, and Y. Deng, Geometric properties of the fortuin-kasteleyn representation of the ising model, *Phys. Rev. E* **99**, 042150 (2019).